Quarterly Progress Report

September 1, 1994 to November, 30, 1994

Visible Light Emitting Materials and Injection Devices

ONR/ARPA URI

Grant Number N00014-92-J-1895

Prepared by:

Paul H. Holloway
Department of Materials Science and Engineering
University of Florida
P.O. Box 116400
Gainesville, FL 32611
Ph: 904/392-6664; FAX: 904/392-4911
E-Mail: Internet-PHOLL@MSE.UFL.EDU

Participants:
University of Florida
Kevin Jones
Robert Park
Joe Simmons
Dept. of Materials Science and Engineering
Tim Anderson
Dept. of Chemical Engineering
Peter Zory
Dept. of Electrical Engineering
University of Colorado
Jacques Pankove
Dept. of Electrical Engineering
Columbia University
Gertrude Neumark
Dept. of Materials Science and Engineering
Oregon Graduate Institute of Science and Engineering
Reinhart Engelmann
Dept. of Electrical Engineering

(I) Molecular Beam Epitaxy Growth of II-VI and III-Nitrides (Robert Park)

(a) Widegap II-VI Work

Some interesting results were obtained this quarter in the area of time-resolved stimulated emission and time resolved lasing in our MBE-grown $Cd_{0.2}Zn_{0.8}Se/ZnSe$ multiple quantum well structures. Dr. Robert Taylor of Oxford University has been able to time-resolve the onset of stimulated emission and of lasing in cavities cleaved from our MQW structures. The cavities were pumped on edge using 100 fs blue light pulses from a frequency doubled Ti: sapphire laser.

Since there are no reports in the literature (as far as we are aware) on time-resolving stimulated emission in widegap II-VI systems, we believe that these results are quite exciting.

We are presently studying the influence of quantum well width in the $Cd_{0.2}Zn_{0.8}Se/ZnSe$ MQW system using time-resolved lasing measurements on the carrier dynamics and lasing behavior where the exciton binding energy is less than and greater than the LO phonon energy. The goal of this work from the project standpoint is to determine an optimum structure for lasing in terms of well and barrier widths, etc.

(b) Column III-Nitride Work

Our focus this quarter was on the growth of GaN by MBE on both a-plane and c-plane sapphire substrates.

Using RHEED analysis, we observed a 6-fold symmetry, c-plane orientation for the GaN films grown on both a-plane sapphire and c-plane sapphire. For the case of the c-plane on c-plane growth, we observed a 30° rotation of the GaN with respect to the sapphire substrate.

HRXD rocking curve analysis indicated FWHM values for the GaN epilayers in the range, 17 to 20 min., for growth on a-plane sapphire (depending on growth conditions) and in the range, 8 to 14 mins., for growth on c-plane sapphire. A low temperature GaN buffer was found to yield smaller rocking curve linewidths than an AlN buffer.

Our best data for rocking curve linewidths are plotted in Fig. I.1 as a function of GaN film thickness along with the literature data. In all cases the GaN films were grown on sapphire substrates (either a-plane or c-plane).

We also performed Hall-effect measurements on a number of GaN/c-plane sapphire samples grown under a variety of conditions. We are investigating the influence of GaN buffer layer thickness and growth temperature, epilayer growth temperature, epilayer thickness and radical source plasma intensity on the electrical properties (carrier concentration and mobility) of the wurtzite GaN material.

Our "best" data point so far is shown in Fig. I.2 along with the literature data.

(II) Ohmic Contact Formation (Paul Holloway)

(a) ZnSe Contacts

Au and Ag contacts were evaporated onto p-ZnSe (N doped with a carrier concentration of $3x10^{17}$ cm^{-3}) and were sequentially heat treated at temperatures of 150, 200, 250, 300,350, and 400°C. At each temperature, the samples were heat treated in 15

Fig. I.1

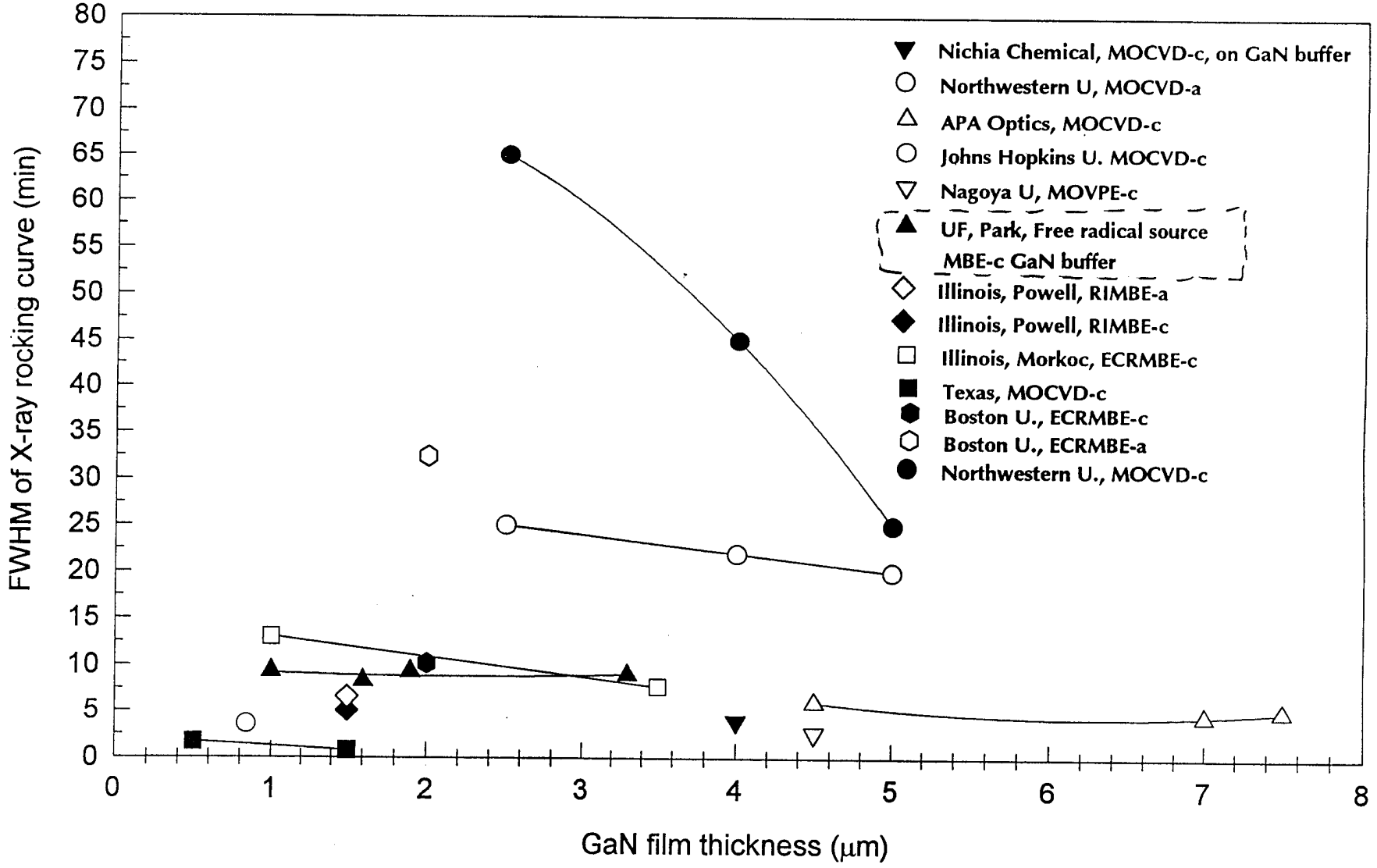
FWHM of X-ray rocking curve (min)
GaN film thickness (μm)
0
5
10
15
20
25
30
35
40
45
50
55
60
65
70
75
80
0
1
2
3
4
5
6
7
8
Nichia Chemical, MOCVD-c, on GaN buffer
Northwestern U, MOCVD-a
APA Optics, MOCVD-c
Johns Hopkins U. MOCVD-c
Nagoya U, MOVPE-c
UF, Park, Free radical source MBE-c GaN buffer
Illinois, Powell, RIMBE-a
Illinois, Powell, RIMBE-c
Illinois, Morkoc, ECRMBE-c
Texas, MOCVD-c
Boston U., ECRMBE-c
Boston U., ECRMBE-a
Northwestern U., MOCVD-c

Fig. I.2

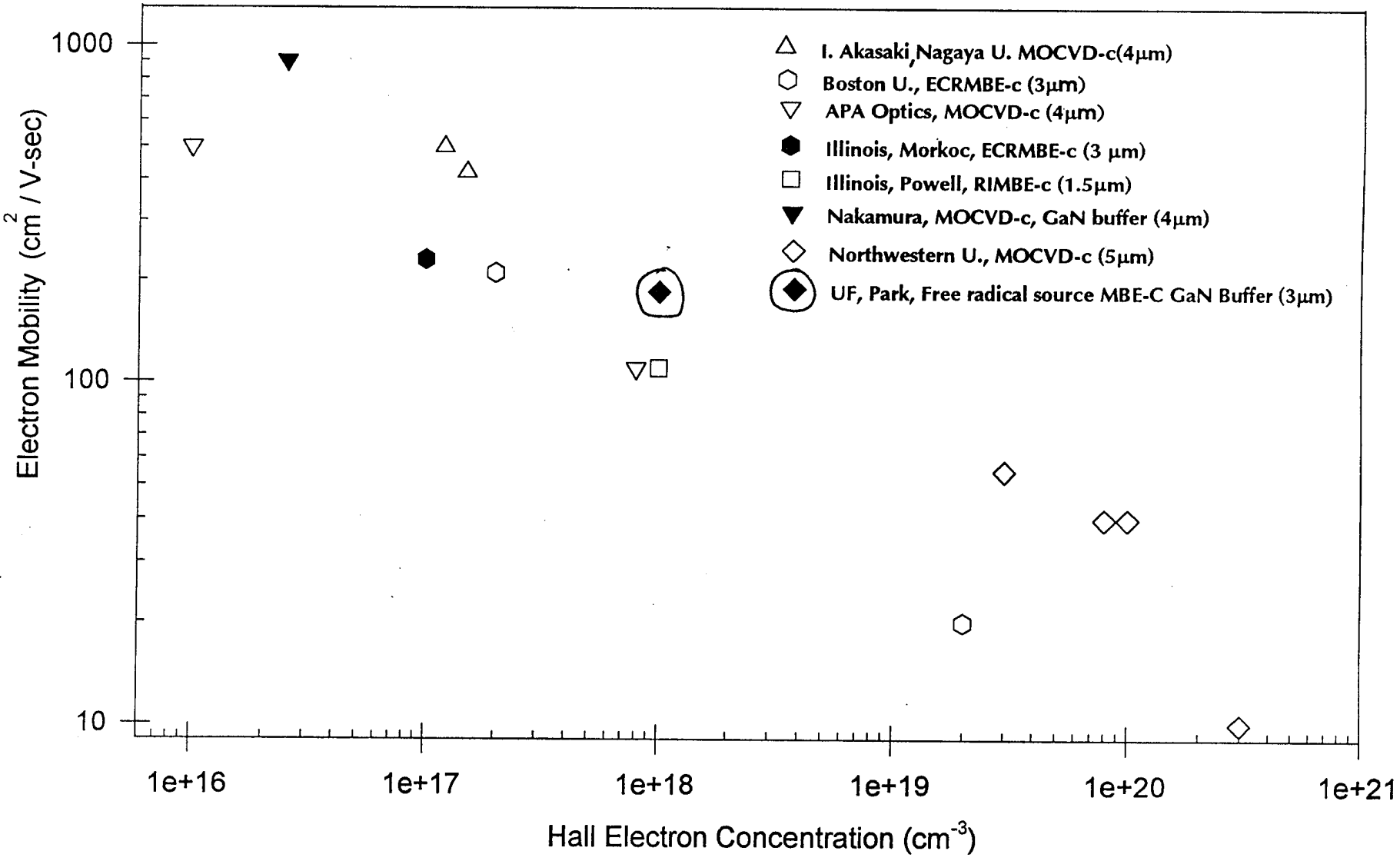
1000
100
10
Electron Mobility (cm^2 / V-sec)
1e+16
1e+17
1e+18
1e+19
1e+20
1e+21
Hall Electron Concentration (cm^{-3})
I. Akasaki, Nagaya U. MOCVD-c(4μm)
Boston U., ECRMBE-c (3μm)
APA Optics, MOCVD-c (4μm)
Illinois, Morkoc, ECRMBE-c (3 μm)
Illinois, Powell, RIMBE-c (1.5μm)
Nakamura, MOCVD-c, GaN buffer (4μm)
Northwestern U., MOCVD-c (5μm)
UF, Park, Free radical source MBE-C GaN Buffer (3μm)

minutes intervals for a total of 90 minutes. The I-V characteristics of the samples were taken following each 15 minutes interval. Previous results from sputter deposited Au and Ag contact indicate that the reverse bias breakdown voltage (RBBV) of Ag contacts is reduced by the presence of interfacial oxygen, resulting in Ag contacts having a lower RBBV than Au contacts. As a result, the evaporated Au and Ag contacts were heat treated in both forming gas (10 % hydrogen, 90 % nitrogen) and oxygen ambients.

Results from the heat treated samples further support that oxygen is resulting in the lower RBBV of Ag contacts. The Ag contacts were found to have a lower minimum RBBV of 2.4 volts for samples heat treated at 150°C in oxygen as opposed to 3.8 volts for samples heat treated at 150°C in forming gas. The RBBV and resistance was found to increase for Ag contacts heat treated between 200 and 350°C in both ambients. However, the resistance and RBBV decreased during heat treatments at 400°C for the sample in oxygen but continued to increase for the sample in forming gas. The Au samples exhibited little difference in RBBV regardless of the ambient used during heat treatment. However, at heat treatment temperatures of 300°C and greater, the resistance of the Au contacts was found to increase faster for samples heat treated in forming gas. This indicates that heat treatment in oxygen results in a lower RBBV for Ag contacts and helps stabilize the resistance of both Au and Ag contacts during high temperature heat treatments.

Other work has focused on studying the degradation caused by high current densities in ZnTe/ZnSe (pseudo-graded or multiquantum well) ohmic contacts to p-ZnSe. Samples with ZnTe/ZnSe ohmic contacts to p-ZnSe were received from Paul Baude at 3M. The samples were grown on p-GaAs, onto which we have deposited Ti/Au backside ohmic contacts. We have also deposited Pt/Au front side ohmic contacts on the ZnTe/ZnSe structure. Software has been written and hardware has been assembled to monitor current, voltage, and temperature during the degradation of the samples. Preliminary data has been collected from several samples.

(b) ZnTe Contacts

Studies of the formation of ohmic contacts to p-ZnTe have continued with emphasis on Au electrical contacts. Gold films (1100 Å) were analyzed using current-voltage (I-V) measurements to determine thermal stability upon post deposition annealing. Auger electron spectroscopy (AES), optical and scanning electron microscopy (SEM), and secondary ion mass spectrometry (SIMS) were used to study composition changes at the interfaces. Non-linear I-V curves were obtained for the as deposited contacts, while the curves became linear and the resistance was lower upon annealing at temperatures greater than 150°C for 15 minutes (Figure II.1). For an optimum anneal of 250°C for 15 minutes, a current density of 2.3 A/cm^2 was obtained at 5 V. The I-V characteristics of the contacts were found to degrade at a temperature of 350°C for a 15 minute anneal (Figure II.2). AES depth profiles were collected from samples annealed for 90 minutes at both 200°C and 250°C. No compound formation was detected at either temperature. SEM micrographs showed an extended reaction zone on the surface around the dot contact after annealing at 250°C. No reaction zone was observed at 200°C. Auger data showed a higher concentration of Au in the 250°C reaction zone. Further SEM and AES work will be done to better understand this surface spreading reaction. SIMS data are presently being collected in an effort to determine diffusion profiles of the annealed samples and also to help in the analysis of the above spreading reaction.

I-V Data for Au/p-ZnTe as Deposited and Annealed 15 min at 150 C

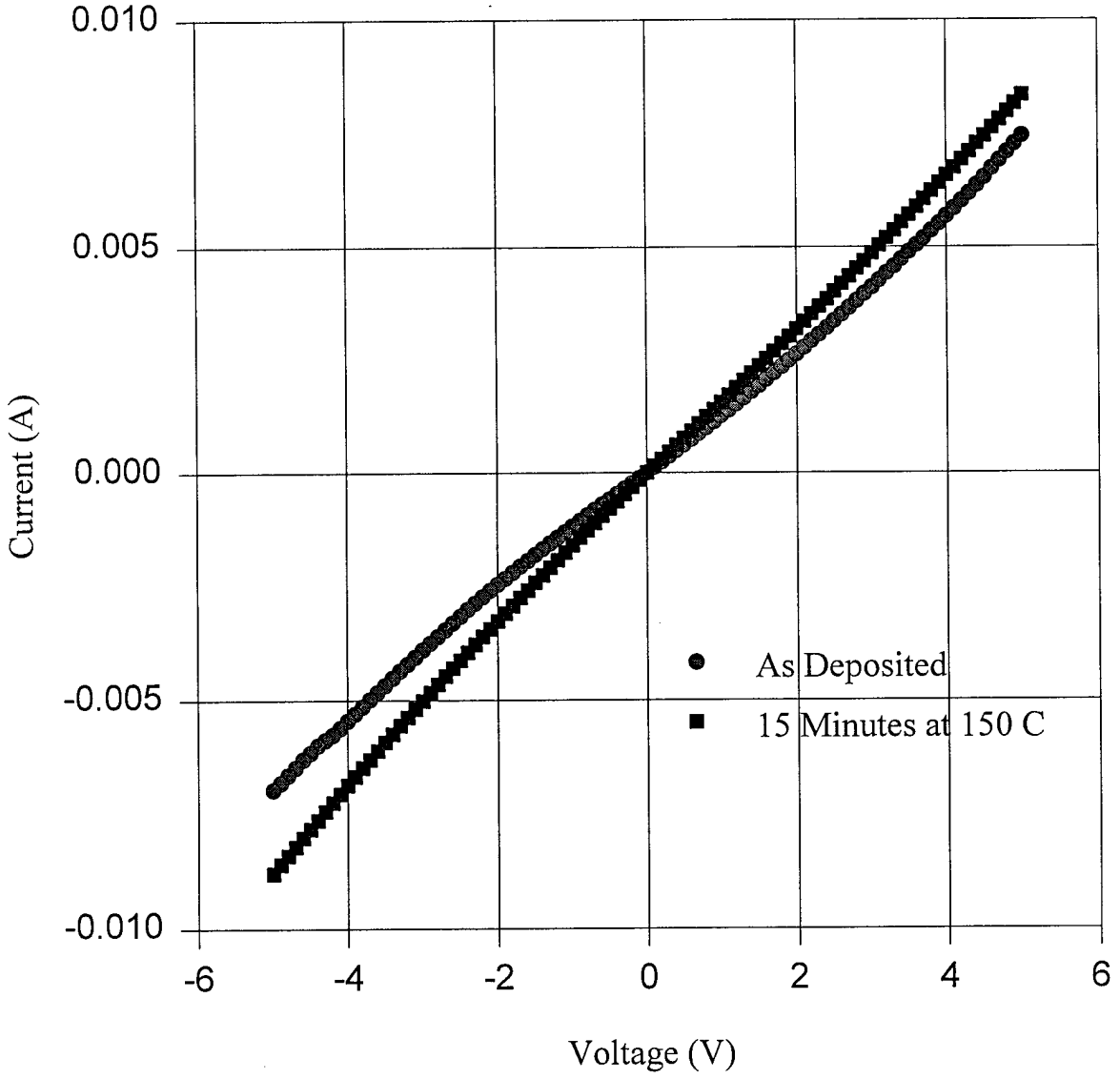

Fig. II.1b

I-V Data for 15 Minute Anneals at Various Temperatures

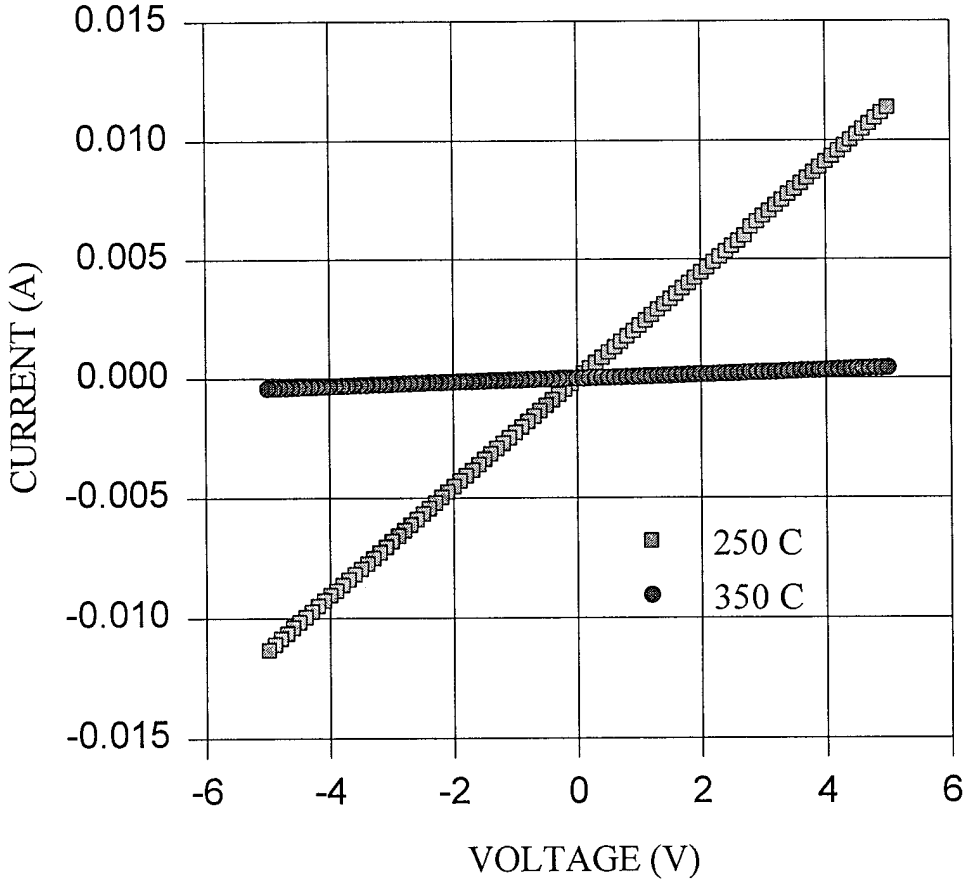

Fig. II.2b

(c) GaN Contacts

The investigation of ohmic contact formation to CVD grown, wurtzite n-type GaN (unintentionally doped, $2x10^{18}$ cm^{-3}) by using Ti/Au (50 nm/200 nm) and Ti/Si/Au (10 nm/100 nm/200 nm) schemes has continued. The current-voltage (I-V) characteristics of these contact schemes were recorded for temperature conditions of 400°C, 500°C, and 600° C for times of 5,15, and 30 minutes in a nitrogen ambient. The contacts were found to be nonlinear in the as deposited condition and remained nonlinear throughout the series of heat treatments. Auger depth profiles performed on the heat treated samples indicated that Ti and/or Si had diffused to the surface during the heat treatments and formed a surface oxide layer that may have increased the contact resistances. In an attempt to impede the interdiffusion of the Au and Ti during the heat treatment process, the contact scheme of Ti/Mo/Au (50 nm/ 400 nm/ 200 nm) was tried for the same n-type GaN samples. I-V results for the as deposited case were less linear than in either the case of the Ti/Au or the Ti/Si/Au. Heat treatments of 400°C, 600°C, and 700°C in a nitrogen ambient were investigated for this metallization as well. Heat treated contacts also had less linear I-V characteristic than for the Ti/Au or the Ti/Si/Au contacts.

An investigation of Au contacts on low pressure-CVD grown p-type GaN (unintentionally doped, $1x10^{16}$ cm^{-3}) on sapphire films, received from APA Optics Inc., has also been started. Au contacts 100 nm thick were sputter deposited onto the p-type GaN. According to theoretical predictions, the gold metal, having a very high work function should make an ohmic contact to the p-type material as deposited. To date, no ohmic contact has been formed on these samples, and only very nonlinear I-V, non-ohmic contacts have been produced. Heat treatments of 200°C and 400°C for up to 30 minutes in a nitrogen atmosphere have been performed. Auger depth profiles and scanning electron microscopy analysis have been performed to characterize the interfacial behavior between the Au and GaN, and to characterize the surface morphology of the Au contacts as well. The results of this analysis will be reported in the future. Finally, we will begin an investigation into the Ni/Au contacts to p-type GaN, while continuing to investigate the Ti/Au and Ti/Si/Au schemes.

(III) Microstructural Analysis of II-VI and III-V Materials (Kevin Jones)

Degradation study of II-VI LEDs

Degradation studies were conducted on the II-VI LEDs by Electroluminescence(EL) microscopy and Transmission electron microscopy (TEM). Two types of samples which have a quantum well (QW) structure grown by molecular beam epitaxy were used for the fabrication of LEDs. The first sample is a separate confinement laser structure with the following growth sequence: n^+ GaAs substrate/ZnSe buffer/n-type ZnSSe/n-type ZnSe/CdZnSe QW/p-type ZnSe/p-type ZnSSe/p-type ZnSe. This structure has a fairly large number of extended defects. The threading dislocation density as measured by TEM is on the order of 10^9 per cm^2. The second type of sample has a different structure: n^+ GaAs substrate/ZnSe buffer/n-type ZnSSe/CdZnSe QW/p-type ZnSSe/ZnSe-ZnTe graded contact. The defect density for this structure is less than 10^6 per cm^2. The LEDs were fabricated from these two different QW laser structures by depositing gold contact pads

(200μm x 200μm and 100 nm thick) with 100 nm thick 50 nm wide gold contact strips around the perimeter.

(a) Degradation behaviors in EL microscopy: EL imaging during LED operation was carried out by passing the light exiting from the surface of the LED through an optical microscope system in order to observe the progress of degradation. For the sample of higher defect density, dark spot defects appeared after only a few seconds of operation, which support the postulate that the pre-existing defects in the structure act as non-radiative recombination centers. These spots became larger and connected together and then finally the whole LED was dark. For the sample of lower defect density, dark line defects (DLD), similar to observations made for GaAs based devices, developed during the operation. These DLDs were propagating from the outer gold stripes to the center area, which implies that either strain in the gold contact or current flowing through the device has an important effect on the degradation.

The changes of output power from LED's were measured under the same driving conditions during degradation. As shown in Fig. III.1, the output power decreased exponentially, depended on the pre-existing defect density, and depended on the current density. The larger the defect density or current density, the faster the output power decreased.

(b) TEM investigation: Cross sectional TEM samples were prepared from the degraded LEDs. It appears that defects which developed during operation are closely related with the pre-existing defects such as stacking faults, misfit dislocations and threading dislocations. One type of newly generated defects were threading dislocations which spans from the surface to the interface between the epilayer and the GaAs substrate. The other type was a group of dislocations parallel to and confined in the QW. It appeared that a main dislocation was generated at the QW region and some branches of dislocations came out of this main dislocation as shown in the TEM image attached (Fig. III.2). The mechanisms of development of those extended defects during degradation is being further investigated.

(IV) Optical and Electrical Characterization of ZnSe (J.H. Simmons)

Summary of past work:

Our research efforts in the past quarter have focused on the study of optical damage in ZnSe films and diode structures, and on the effect of growth temperature on film quality.

1. Optical degradation studies:

The research has followed the objective of inducing damage in films and evaluating its consequence on film characteristics, particularly structural (Kevin Jones) and optical properties. The rationale is that in-use damage arises from the strains developed by the induced current in the structures. We have selected to work with externally induced optical damage in order to have the flexibility of studying separately each layer in the diode structure. Since it is clear that the initial structural damage is formed in the buffer layers and spreads to the active layer during use, this approach allows us to examine the buffer layers independently, and better assess the conditions for spread of structural damage.

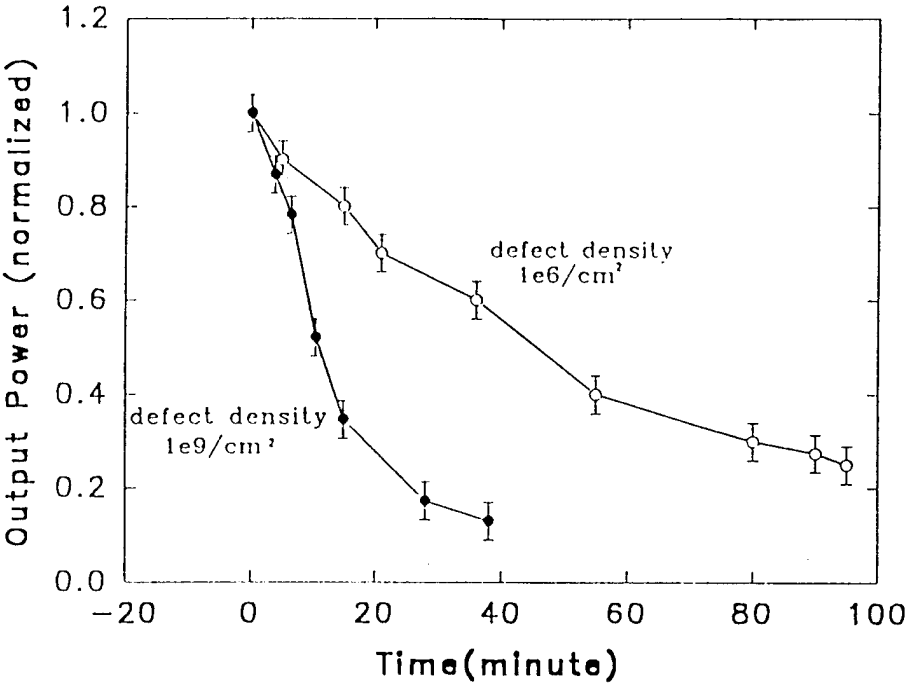

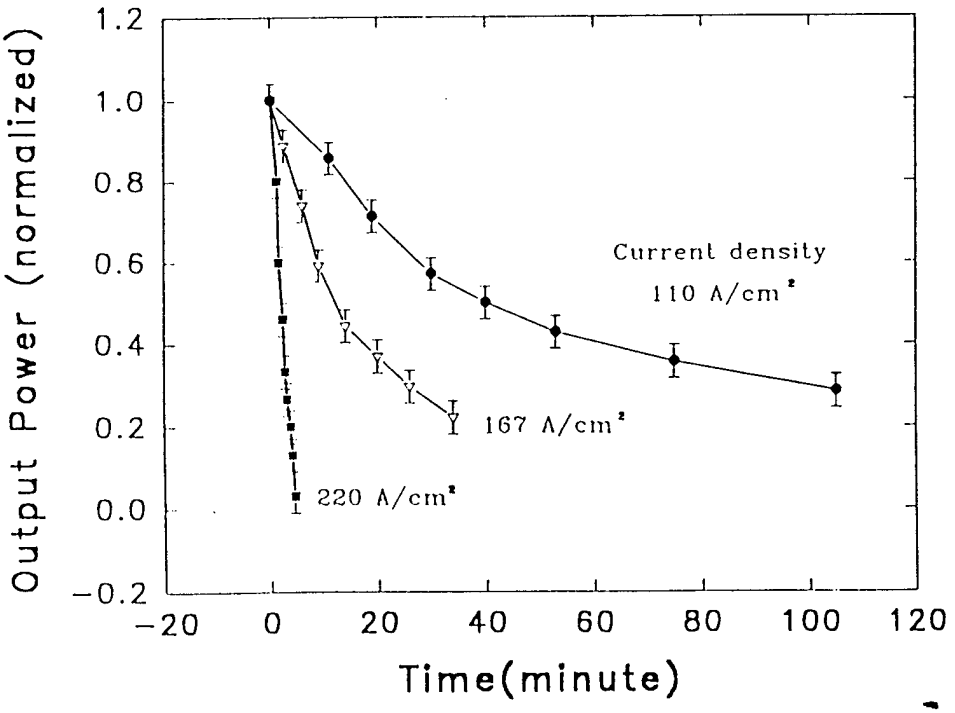

Fig. III.1. Degradation Dependence on Pre-existing Defect Density and Driving Current Density.

XTEM Characterization

As Grown Structure

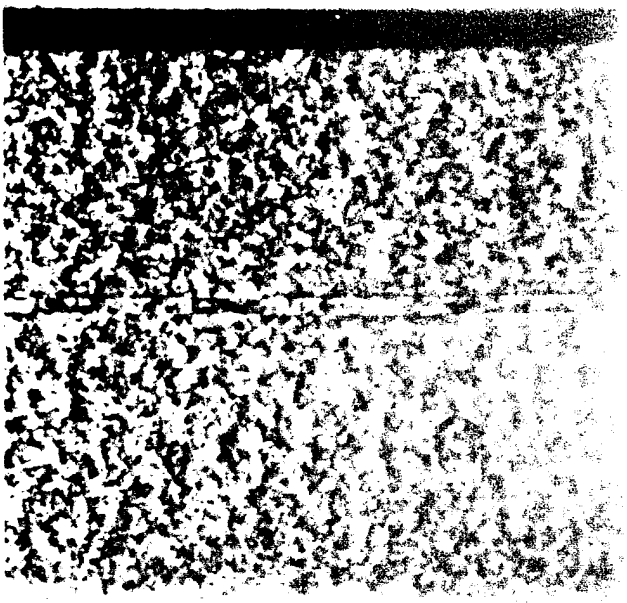

ZnTe/ZnSe
graded contact

N: ZnSSe

ZnCdSe Q.W.

Cl: ZnSSe

GaAs Substrate

Electrically Degraded to 30 % EL

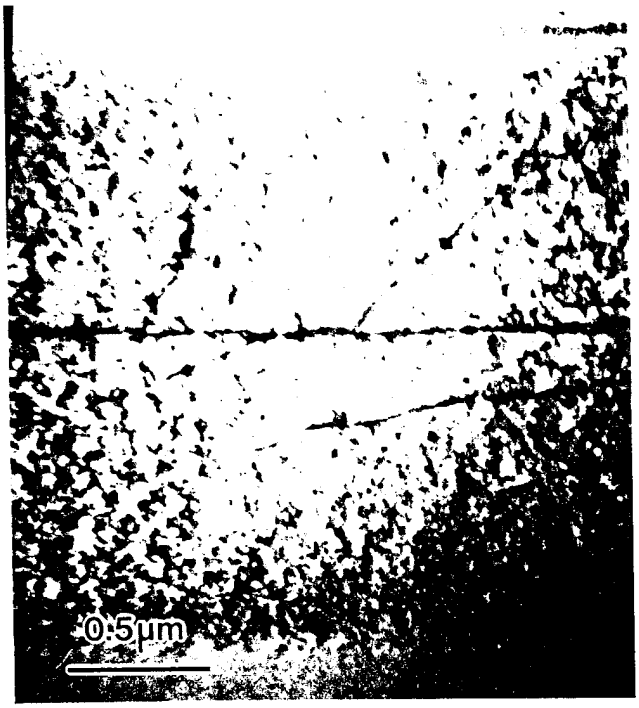

Driving Current : 167 A/cm^2
Rep. Rate : 10 KHz
Duty Cycle : 40 %

Fig. III.2

Damage was induced in films and diode structures by exposing them to optical radiation from a pulsed nitrogen laser beam and a doubled Ti-sapphire laser beam. The nitrogen laser operates at 337 nm with pulses of 2.5 mJ over 600ps at a repetition rate of 5 Hz. With an optical density of 1W in the first micrometer, this corresponds to a current density of $2x10^{21}$ carriers/cm^{-3}-sec. A diagram for the test set-up is shown in Figure IV.1. The doubled Ti-sapphire laser operates at 400 nm, with pulses of 26 pJ over 300 fs at a repetition rate of 76MHz. This corresponds to a current density of $4x10^{20}$ carriers/cm^{-3}-sec.

During and following exposure, population mixing (PECS) experiments (Figure IV.2) are conducted on the films to determine associated changes in photoluminescence intensity and in photoexcited carrier lifetimes. This is followed by TEM studies of the structure of films after varied exposures to the optical damage.

Preliminary results show a rapid loss in PL intensity after exposure to the nitrogen laser radiation (Figure IV.3) and to the Ti-sapphire laser (Figure IV.4). Damage from the nitrogen laser is more rapid, despite the low repetition rate of the laser, and is due to the higher current generated in the films. PECS measurements of the diodes exposed to the Ti-sapphire laser show a gradual decrease in free carrier lifetimes. This is shown in Figures IV.5 and IV.6. The latter plots the free carrier lifetime as a function of exposure time and indicates a decrease from about 500 fs to 200 fs in free carrier lifetime. The saturation at 200 fs is very significant, indicating that the photo-induced damage introduced at the current densities of the Ti-sapphire exposure does not completely destroy the films. In fact the PL data (Figure IV.4) only shows a decrease by a factor of 2.5, while the nitrogen laser exposure, because of the larger current density in the film, causes a more severe degradation.

2. Substrate temperature growth studies

This study is described in more detail by Robert Park. Enclosed is a figure (Figure IV.7) showing the difference in PL intensity caused by 3 different substrate temperatures during growth. It is obvious that the 320°C growth produces better films.

(V) MOCVD Growth of MgZnCdS Thin Films (Tim Anderson)

As previously reported, a series of growth studies of $Cd_xZn_{1-x}S$ on GaAs was directed at reducing the extended defect density in this wide bandgap semiconductor. As a result of this comprehensive study, we were able to grow films with the lowest reported FWHM using organometallic group II source with H_2S. The dislocation density, however, was still relatively high. The optimum conditions included growth at the maximum temperature at which deposition occurred (550°C). Above this temperature no growth occurred, presumably due to upstream deposition. For these reasons, a new sulfur source - methyl mercaptan (MSH) - was investigated.

As an initial study MSH was used as the sulfur source for the deposition of pure ZnS on Si (closely lattice matched). Compared to the conventional H_2S source, the growth temperature was increased to as high as 650°C. The optimum conditions for producing ZnS films on Si(111) and (100) oriented substrates were as follows: T=600°C, [Zn]=$1*10^{-4}$ mole fraction and a gas phase inlet VI/II ratio of 60. The growth rate at these conditions was

Fig. IV.1

DIODE DEGRADATION STUDY EXPERIMENTAL SETUP

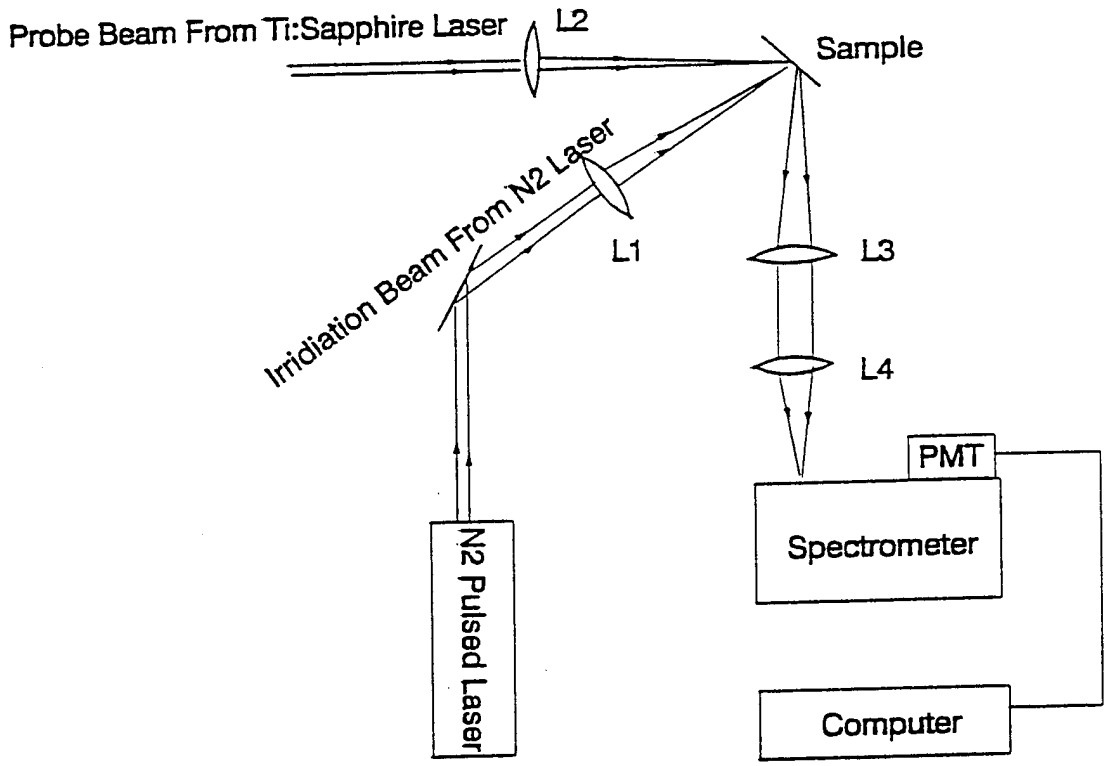

Fig. IV.2

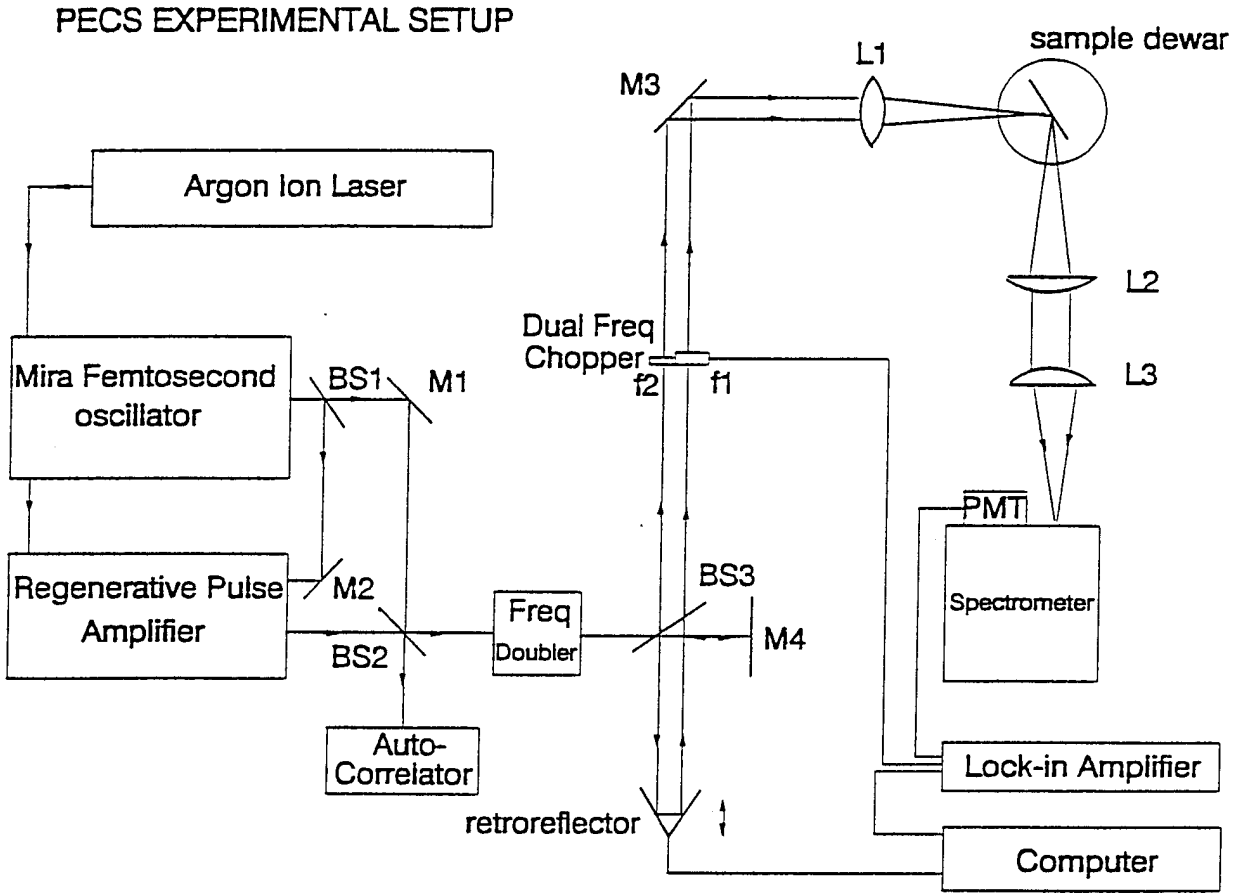
PECS EXPERIMENTAL SETUP
sample dewar
L1
M3
Argon Ion Laser
L2
Dual Freq
Chopper
f2
f1
L3
Mira Femtosecond
oscillator
BS1
M1
PMT
Regenerative Pulse
Amplifier
M2
BS3
Freq
Doubler
Spectrometer
BS2
M4
Auto-
Correlator
Lock-in Amplifier
retroreflector
Computer

Fig. IV.3

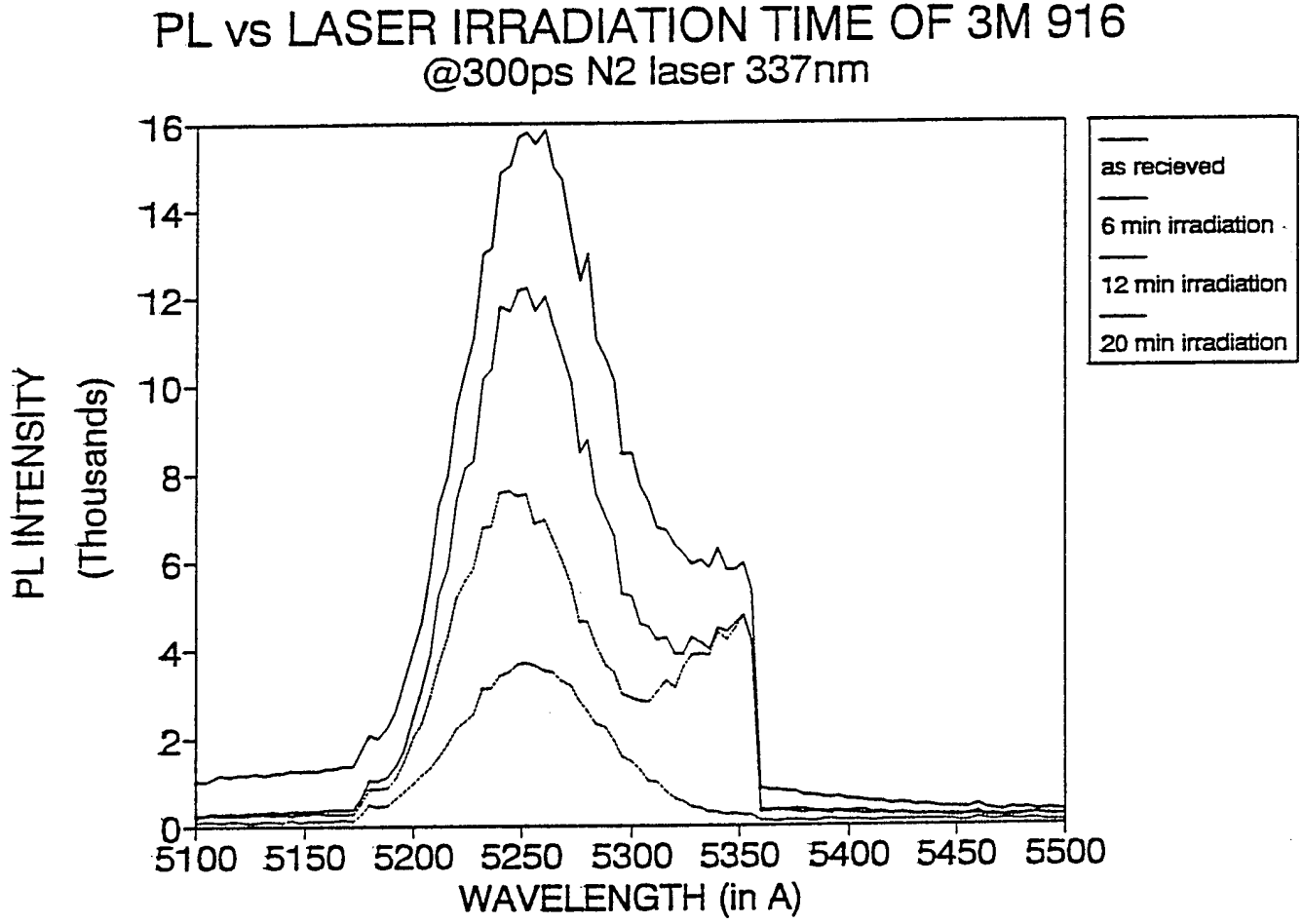
PL vs LASER IRRADIATION TIME OF 3M 916
@300ps N2 laser 337nm
PL INTENSITY
(Thousands)
16
14
12
10
8
6
4
2
0
5100 5150 5200 5250 5300 5350 5400 5450 5500
WAVELENGTH (in A)
as recieved
6 min irradiation
12 min irradiation
20 min irradiation

Fig. IV.4

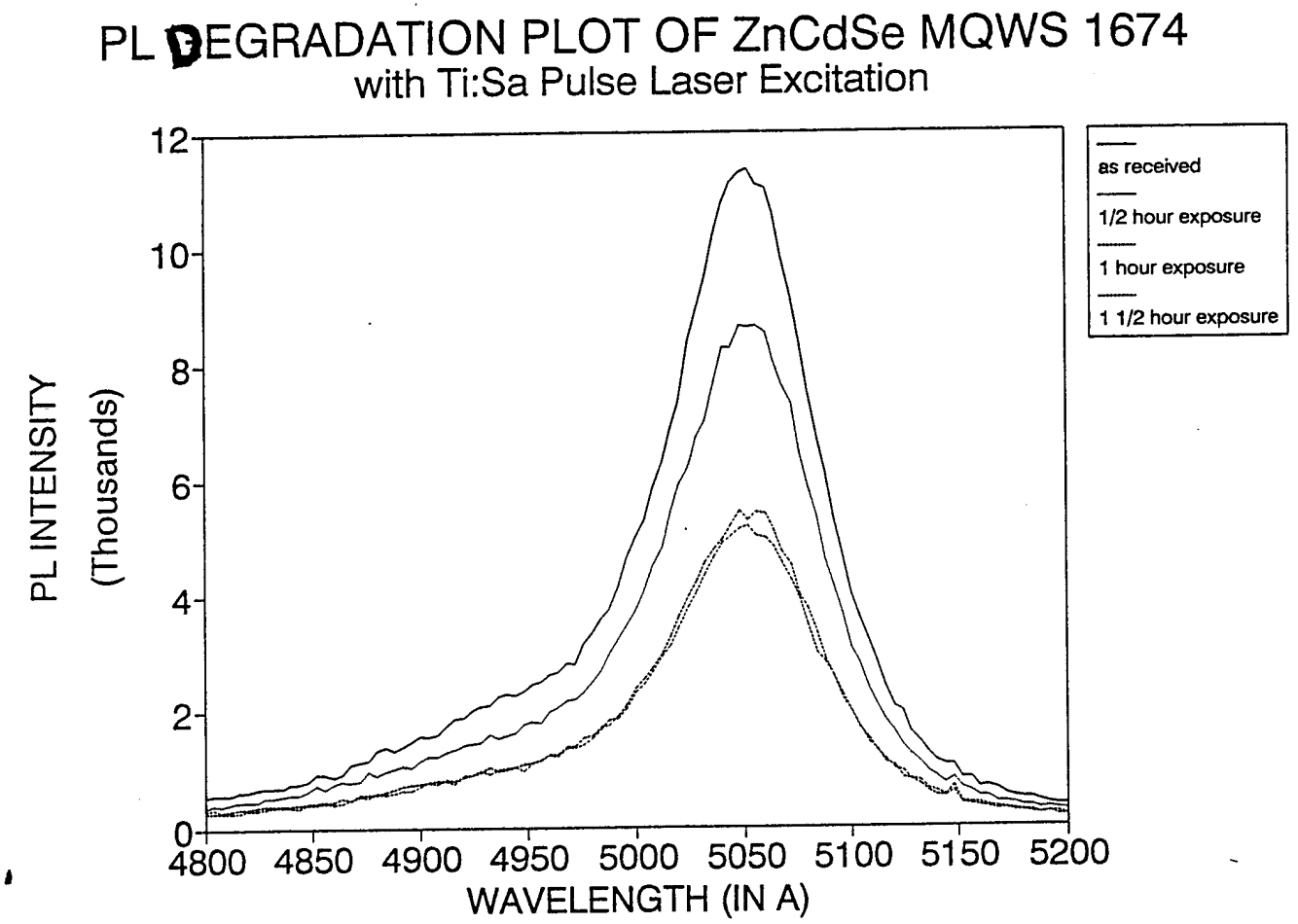
PL DEGRADATION PLOT OF ZnCdSe MQWS 1674
with Ti:Sa Pulse Laser Excitation
PL INTENSITY
(Thousands)
12
10
8
6
4
2
0
4800 4850 4900 4950 5000 5050 5100 5150 5200
WAVELENGTH (IN A)
as received
1/2 hour exposure
1 hour exposure
1 1/2 hour exposure

Fig. IV.5

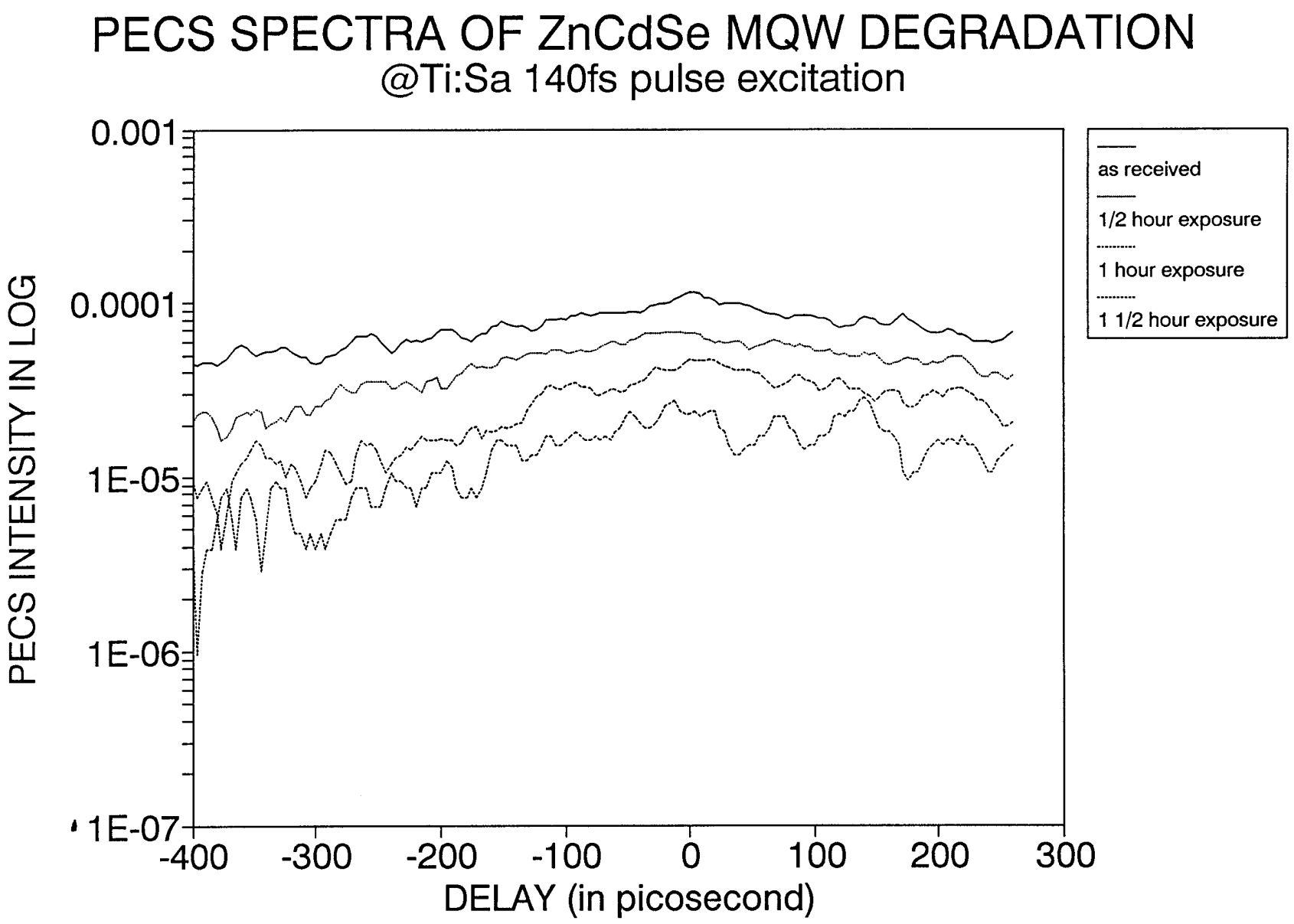
PECS SPECTRA OF ZnCdSe MQW DEGRADATION
@Ti:Sa 140fs pulse excitation
PECS INTENSITY IN LOG
0.001
0.0001
1E-05
1E-06
1E-07
-400
-300
-200
-100
0
100
200
300
DELAY (in picosecond)
as received
1/2 hour exposure
1 hour exposure
1 1/2 hour exposure

Fig. IV.6

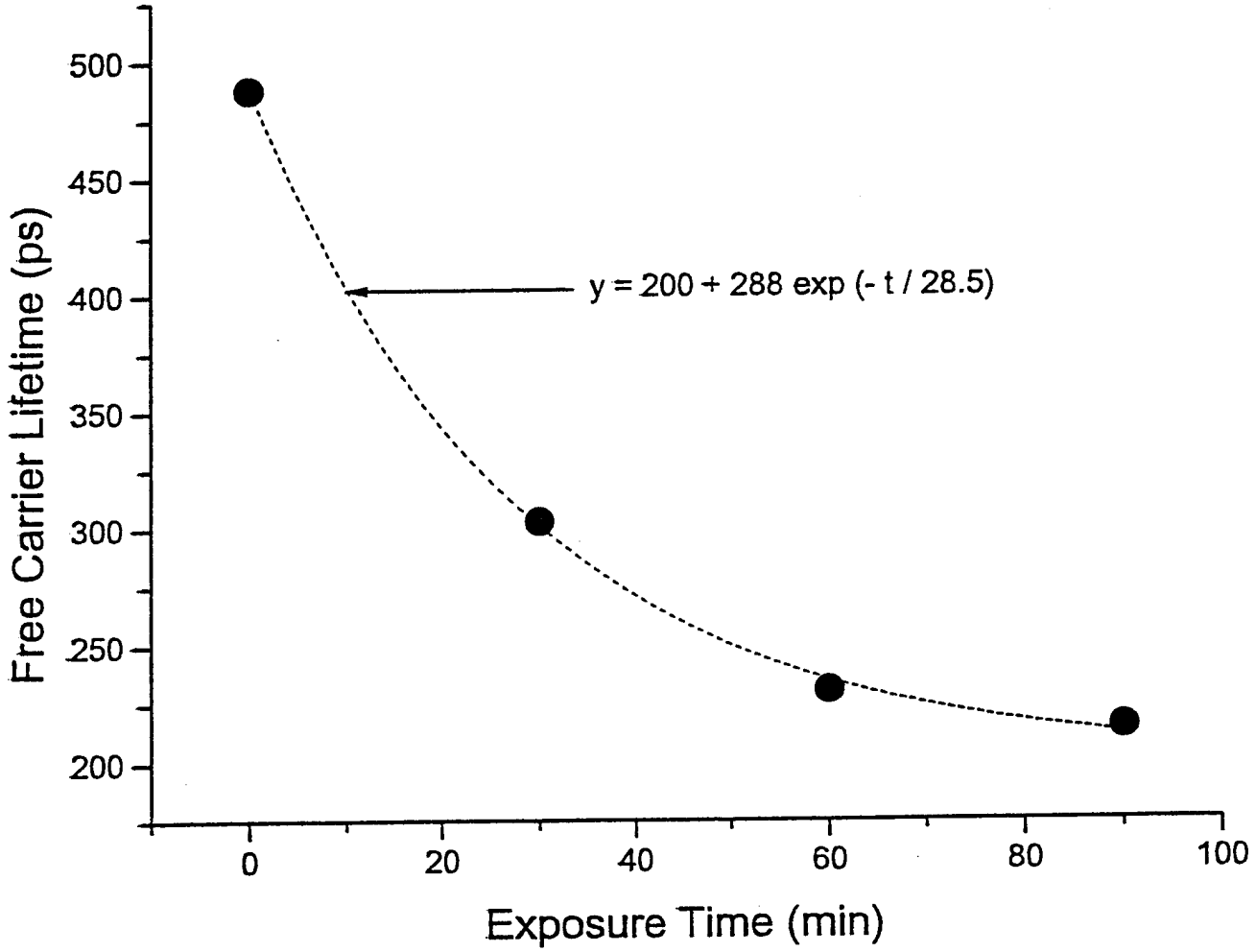
Free Carrier Lifetime (ps)
500
450
400
350
300
250
200
y = 200 + 288 exp (- t / 28.5)
0
20
40
60
80
100
Exposure Time (min)

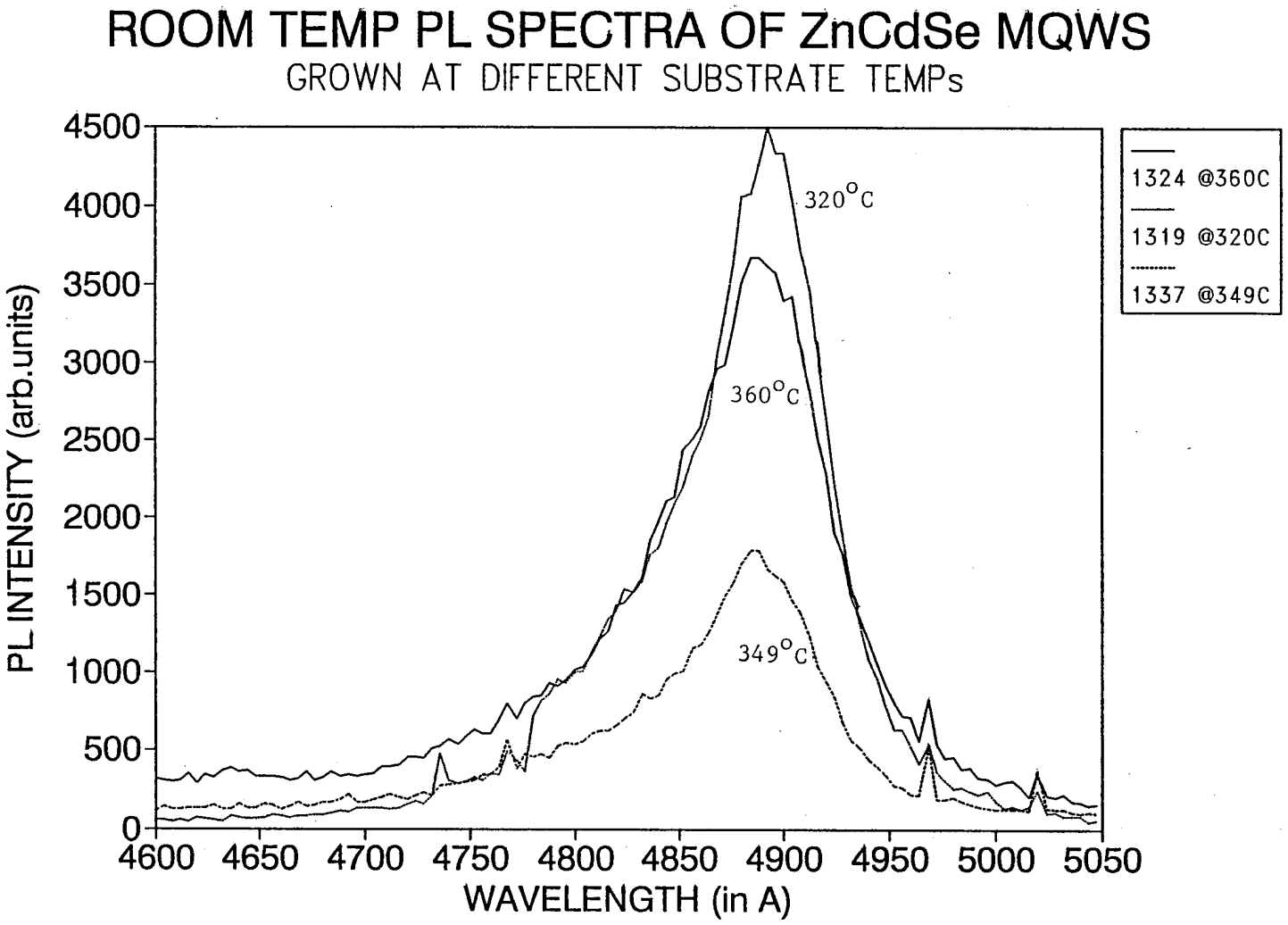
ROOM TEMP PL SPECTRA OF ZnCdSe MQWS
GROWN AT DIFFERENT SUBSTRATE TEMPs
PL INTENSITY (arb.units)
4500
4000
3500
3000
2500
2000
1500
1000
500
0
4600 4650 4700 4750 4800 4850 4900 4950 5000 5050
WAVELENGTH (in A)
320°C
360°C
349°C
1324 @360C
1319 @320C
1337 @349C

Fig. IV.7

approximately 1 μm/hr. The measured FWHM for (111) reflection of ZnS on Si(111) was 370 arc sec.

Initial growth of $Zn_{1-x}Cd_xS$ solid solutions on GaAs and Si substrates were performed using the MSH source. Growth at 550°C with [Zn]/[Cd]= 1:1 and VI/II ratio of 60 yielded a film with a composition of 6 mole % Cd. The crystallinity as characterized by HRXRD yielded a FWHM of 900 arc sec for the (400) reflection on GaAs(100) substrate. This is compared to 2000 arc sec for the films produced from H_2S source under similar growth conditions. Further efforts to optimize growth conditions for the $Zn_{1-x}Cd_xS$ films are continuing using the new sulfur source.

Another approach to improving the crystallinity of the films is to deposit low temperature buffer layer material with a closely matched lattice parameter to the GaAs substrate prior to the growth of $Zn_{1-x}Cd_xS$. This has been shown to be effective for many binary and ternary III-V systems. The conditions for deposition of $ZnS_{1-y}Se_y$ buffer layer have been studied and the results are shown in Fig. V.1 and V.2. It is seen from these figures that the Se distribution coefficient is much greater than unity. This is indicative of the higher decomposition temperature for the S versus the Se sources or nonideality in the solid solution behavior. A buffer epilayer of $ZnS_{1-y}Se_y$ of about 1 μm in thickness was grown at 400°C with a composition matched to GaAs(100). A FWHM of 250 arc sec for the (400) reflection was produced at a gas phase S/Se ratio of about 0.3 to 0.4.

Based on the optimum conditions found for the $ZnS_{1-y}S_y$ buffer layer deposition, growth of $Zn_{1-x}Cd_xS$ utilizing the new MSH source will be attempted on thin low temperature ZnS_ySe_{1-y} buffer layers.

MOCVD Growth of GaN Films

The goal in this quarter has been to investigate the effect of growth temperature on the growth rate of GaN thin films. This aspect of the research will enable us to identify the temperature regions of three major reaction mechanisms: thermodynamics, kinetics and hydrodynamics that govern a typical MOCVD reaction process. In this study, we have determined the growth temperature regimes for the range from 650°C to 850°C. The results are illustrated in Table 1. Ammonia and triethylgallium were used as reactant precursors, while Al_2O_3 (0001) and 6H-SiC (0001) were employed as substrates. Prior to each deposition, a low temperature GaN buffer layer was grown at 600°C. The films were grown at a constant V/III ratio and gas velocity. The samples were characterized by Nomarski microscopy, powder X-ray diffraction (XRD) and Sloan Dektak II thickness profiler.

The GaN films were epitaxial and hexagonal in structure as determined by XRD (Table 1). All films showed full and uniform coverage on the substrates, however the growth rate varied depending on the type of the substrates. The growth rate varied from 74 to 130 A/min for films on Al_2O_3 while it varied from 83 to 167 A/min for films on 6H-SiC when the growth temperature was changed from 650 to 850°C. The peak growth rate was obtained (167 A/min) on 6H-SiC substrate at 750°C but no leveling off was observed. However, the growth rate has leveled off in the 700 to 800°C range on Al_2O_3 substrates indicating a distinct mass transport region. This means, the kinetic and thermodynamics zones are in the vicinity of <700°C and >800°C, respectively, as the growth rates drop in those regions. The growth appears to vary slightly (83 to 102 A/min) across the 750°C temperature zone for films deposited on 6H-SiC substrates. It seems that a narrow mass transport region may exist

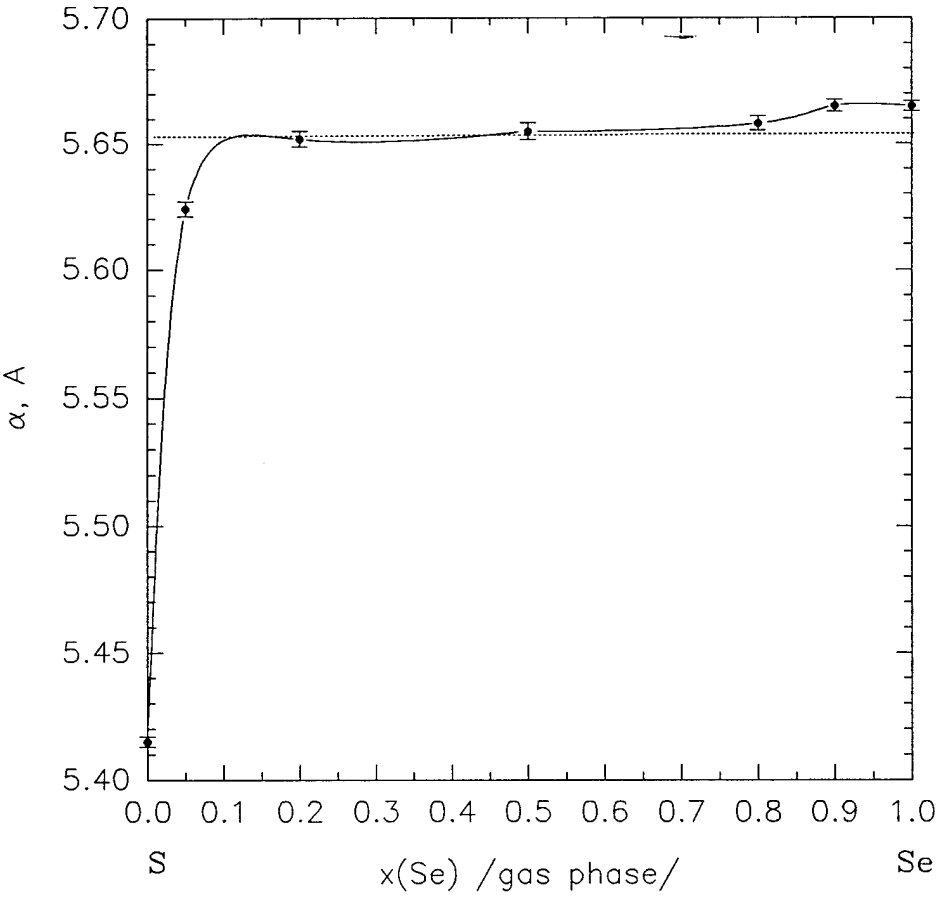

Fig. V.1. Lattice parameter of $ZnS_{1-x}Se_x$ films as function of a gas phase composition.

Growth conditions: t=400 C, VI/II inlet ratio is 80.

(Dashed line corresponds to the lattice parameter of GaAs).

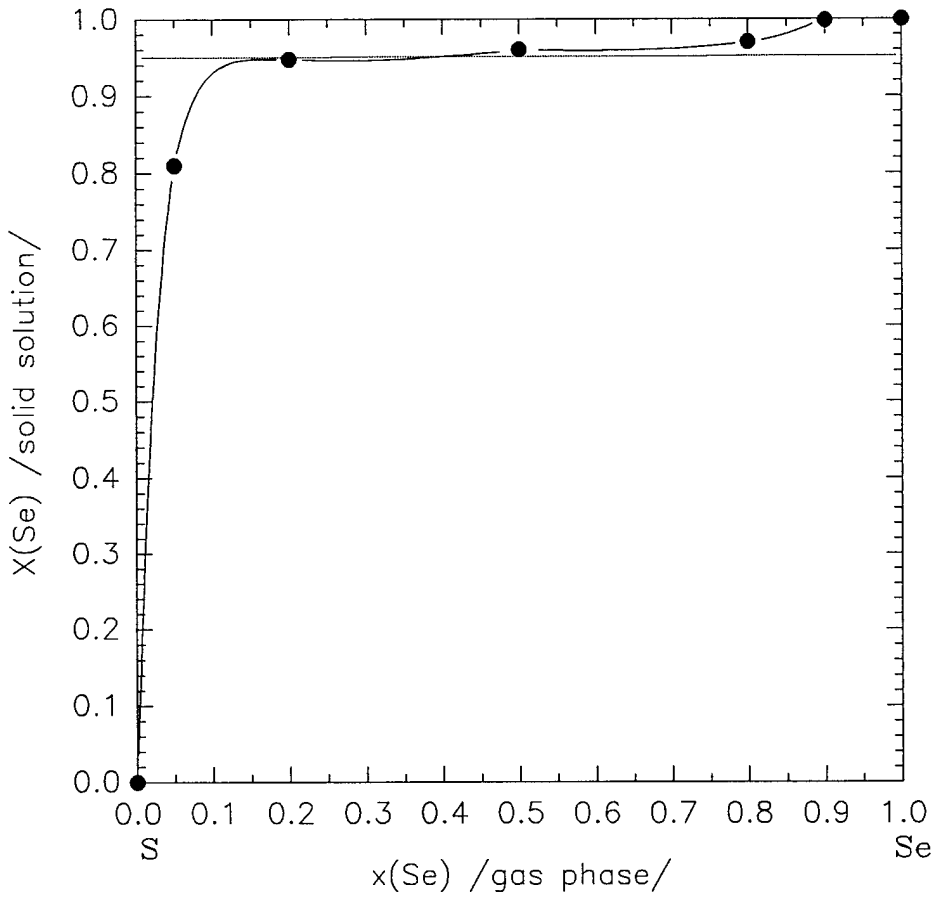

Fig. V.2. Composition of $ZnS_{1-x}Se_x$ films as function of a gas phase composition. Growth conditions are the same as on Fig.1. (Dashed line indicates composition of the film lattice-matched to GaAs).

in the vicinity of 750°C. Further work is currently underway to determine these reaction mechanisms.

Table 1.

Sample ID#	Temperature (oC) buffer/epi-layer	XRD	Growth rate (oA/min)		surface Coverage
			GaN/Al2O3	GaN/6H-SiC	
GN54	600oC/850oC	Hexagonal	74	87	Full
GN56	600oC/800oC	Hexagonal	120	83	Full
GN57	600oC/750oC	Hexagonal	125	167	Full
GN58	600oC/700oC	Hexagonal	130	97	Full
GN59	600oC/650oC	Hexagonal	105	102	Full

(VI) Development of Diode Lasers (Peter Zory)

A. Photopumping

The 337 nm nitrogen laser has been repaired and quality evaluation of GaN-based films grown by MOCVD in Dr. Anderson's lab is continuing.

B. Diode Pumping

A new electro-chemical technique has been developed which enables one to "pump" diode material without the need to deposit metal contacts. The technique is non-destructive and has been used to obtain the equivalent of PL spectra at room temperature from CdZnSe strained QW laser material provided by 3M. We believe the technique can be developed into a tool more useful than PL for evaluating diode material at room temperature since it utilizes majority carrier injection into the active region to obtain light emission.

C. Degradation

(1) Degradation studies of 3M laser material are continuing in collaboration with Dr. Jones and students. Dark line defects characteristic of relatively low time-zero defect density material have been generated and TEM analysis is continuing.

(2) We have demonstrated that ZnTe/ZnSe graded contact layers on standard ZnSe based laser material can be anodically oxidized at room temperature. We believe the

resulting oxide has very low stress and may be important in learning how to fabricate long-lived II-VI lasers.

(VII) Theoretical Calculations of Dopants of ZnSe (Gertrude Neumark)

As mentioned previously, work in the literature [K.A. Bowers et al., J. Electr. Mat. 23, 251 (1994)] has reported a change, with temperature, in the optical activation energy of the N acceptor, and explained this by assuming the N acceptor to be located interstitially. An interstitial location implies high ion mobility, which is cause for concern. We therefore decided to check whether the change in activation energy can be explained by a temperature dependent screening, since screening is known to cause a change in activation energy [Neumark, Phys. Rev. B 5, 408 (1972)]. If screening is the cause, there is no need to invoke an interstitial location.

We had previously fit the Bowers et al. data with "reasonable" parameter values, up to about 180 K. We have since obtained the electrical parameters measured for the sample on which Bowers et al. give detailed optical data [Z. Yang et al., Appl. Phys. Lett. 61, 271 (1992)]. Screening parameters obtained from this electrical data gave an excellent fit, to the optical data from 100 (the lowest optical point is at 89 K) to 160 K, and a reasonable fit at 180 K; this is shown in Figure VII.1. The fit at higher temperatures is not good, but this could be due to other factors, such as excited states.

As part of our investigation of screening in explaining the optical data, we also checked its role in the interpretation of electrical measurements. Preliminary results indicate that the inclusion of screening effects may appreciably increase compensation ratios evaluated from the data by standard means (i.e. without including a temperature dependence of the activation energy), by factors of 2 or more. However, we have to check the accuracy of our relatively simple screening approximations before reaching definitive conclusions.

Additional work has been performed on preferential donor-acceptor pairing. We have shown that strong (i.e. observable) pairing requires a high ion mobility, where one member of the pair must be mobile to about 500 K or lower. We have also evaluated literature data for evidence of such pairing involving deep (compensating) donors formed in heavily N-doped ZnSe. We concluded that there are definite indications of such pairing, but that one cannot prove such pairing from presently available data. This work has been accepted by Proc. SPIE.

(VIII) MOCVD Growth of GaN (Jacques Pankove)

Our objective is to grow GaN p-n junctions that will be the basis for short wavelength emitters and lasers.

Most of the work this quarter has centered on optimization of the two growth systems. The main emphasis was to separate the two systems so that each reactor has its own gas sources and can run independently and in parallel. In system I (the *vertical* cold-wall MOCVD reactor), recent modification of the reactant gas delivery produced the best quality material we have grown thus far. This GaN film had an electron mobility of 212

Fig. VII.1

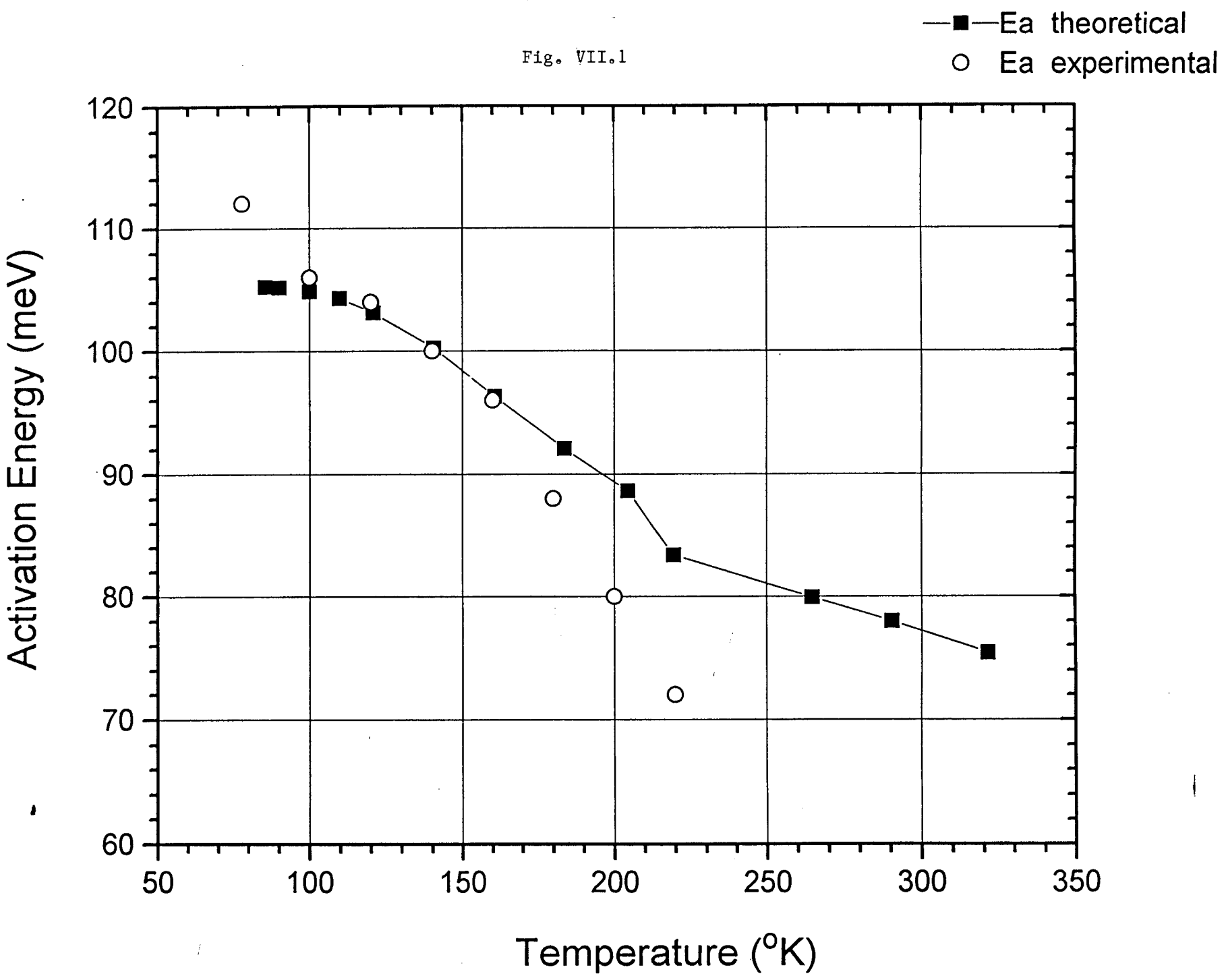
Ea theoretical
Ea experimental
Activation Energy (meV)
120
110
100
90
80
70
60
50
100
150
200
250
300
350
Temperature (°K)

cm^2/Vs and an electron concentration of 8.5×10^{17} cm^{-3}. It was grown without the use of a low temperature buffer layer and further optimization, including the refinement of the buffer layer technique, seems promising. The next step after the mastery of the growth of consistently high quality n-type GaN, is the introduction of Mg as a p-type dopant and the production of p-n junctions.

The reactant delivery manifold of the second system (*horizontal* cold-wall MOCVD reactor) has been extensively modified and extended, now providing five organometallic sources as well as SiH_4 for n-type doping. We have installed four organometallic sources including bis-cyclopentadienalmagnesium (Cp_2Mg), diethylzinc (DEZ), triethylaluminum (TEA), and triethylgallium (TEG). The fifth reactant source will be either trimethylindium or triethylindium. With these reactant gases, we will have the capability of growing both n-type and p-type material as well as ternary alloys of $Al_xGa_{1-x}N$ and $In_yGa_{1-y}N$ for use in double heterostructure and quantum well devices.

In addition to the continued emphasis on the two growth systems, we have expanded the scope of the photoconductivity measurements reported in the previous report. We have measured the temperature dependence of photoconductivity of several GaN samples, both Mg doped and undoped. Although we are still in the process of evaluating the data, some preliminary results are shown in figure VIII.1.

(IX) Gain Modeling in II-VI Strained-Layer QW Structures (Reinhart Engelmann)

Summary

Elastic moduli of both wurtzite and zinc-blende GaN have been obtained for the future strain effect and gain modeling in GaInN/AlGaN strained QW structures. Impurity conduction of p-type wide band gap materials (GaN, ZnSe) has been studied theoretically and appropriate experimental work is being proposed.

1. Elastic Tensors of Wurtzite and Zinc-blende GaN.

The elastic moduli C_{ij} of wurtzite (WZ) GaN are available [1] which have been calculated from the mean square displacement of the lattice atoms measured by X-ray diffraction. These WZ values can be transformed to zinc-blende following the method of R. M. Martin. [2]

The values (in 10^{11} dyn cm^{-2}) are summarized below:

Wurtzite : $C_{11} = 29.6$, $C_{33} = 26.7$, $C_{12} = 13.0$, $C_{13} = 15.8$, $C_{44} = 2.41$, $C_{66} = 3.0$

Zinc-blende : $C_{11} = 23.4$, $C_{12} = 17.0$, $C_{44} = 6.37$.

Other parameters needed for strain effect modeling are hydrostatic deformation potential, shear deformation potential and valence band parameters under strain (Luttinger parameters), which, at present, are still not available.

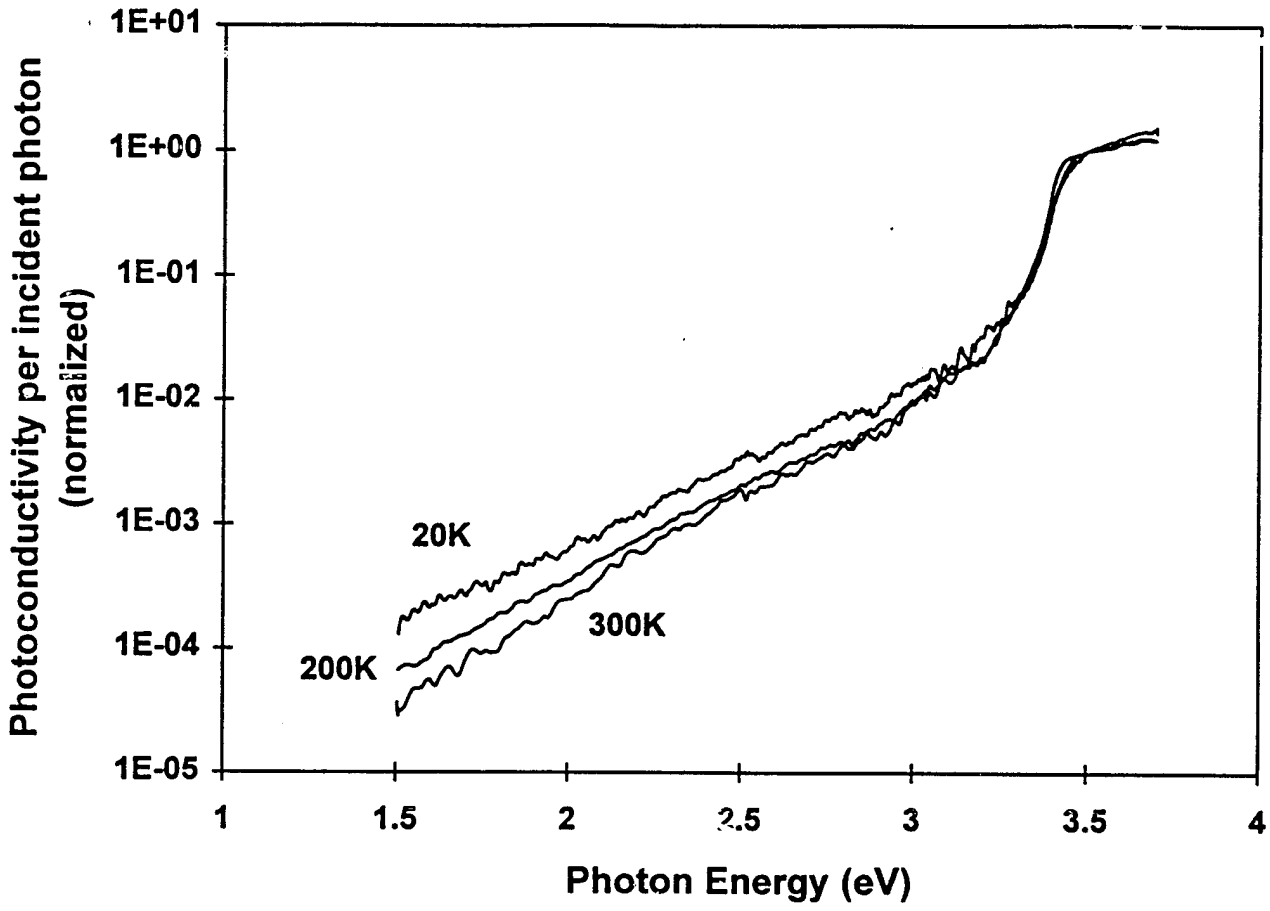

Fig. VIII.1. Photoconductivity spectra of undoped GaN at various temperatures showing the change in slope of the exponential tail.

2. Impurity Conduction of p-Type Wide-Band-Gap Materials

In order to model the carrier transport in wider band gap materials, especially in the p-type layer, we have reviewed the impurity conduction theory (for detail see for example, Mott and Twose [3]).

Impurity conduction originates from the fact that there is a small but finite overlap of the wave function of an electron (or hole) from one donor (or acceptor) center with wave function from neighboring donors (or acceptors). Thus, a conduction process is possible in which the electron (or hole) moves between centers by tunnel effect without activation into the conduction band.

As the concentration N of impurities increases, the activation energy for conduction in the temperature range for impurity conduction decreases and at a critical value Nc vanishes. The Nc can be roughly estimated by

$$N_c = (2.2\ \alpha_H)^{-3} \exp[-(\epsilon-1)]$$

where α_H is the hydrogenic Bohr radius and ϵ is static dielectric constant of the pure host material. (For example for GaN one obtains $N_c \sim 1.2\text{x}10^{20}$ cm^{-3}, for ZnSe, $N_c \sim 8\text{x}10^{20}$ cm^{-3}. For values $N > N_c$ the resistivity and Hall constant are roughly independent of temperature (region of metallic conduction). The overlap of the wave functions is so strong in this case that an impurity band has been formed. Near the transition concentration N_c, an impurity band is formed from donor (acceptor) wave functions, but this band is not yet overlapping the host conduction (valence) band. In this critical situation, the impurity conductivity is very sensitive to the change of the impurity doping level.

In case of p-doping GaN with Mg, the solubility of Mg in GaN seems to be fairly high. An impurity doping level as high as 1.5-5 x10^{20} cm^{-3} has been reported [4]. It is interesting to notice in this context that the metallic form of Mg also has a hexagonal close-packed structure and the lattice constants are a = 3.21 Å, c = 5.21 Å, which are very close to those of GaN (a = 3.19 Å, c = 5.18 Å). This could explain the high solubility. We have estimated the average distance d between the Mg acceptors, at N = 1x10^{20} cm^{-3}, to be d = 21 Å, and at N = 5x10^{20} cm^{-3}, d = 12.6 Å. Thus, we believe that an impurity band is very likely formed in p-type GaN.

The low turn-on voltage and the discrepancy of the reported acceptor level between the thermally measured value 0.15 - 0.2 eV and the optically measured value 0.5 - 0.6 eV can be understood by the impurity conduction model.

In case of N doped ZnSe, the solubility of N seems limited to about 10^{19} cm^{-3}. So the impurity level is below N_c. This could be the reason that the turn-on voltage of ZnSe based device is much higher than GaN based device.

In a GaN based device, on the other hand, the impurity band might cause a carrier confinement problem, because it effectively shrinks the band gap. Considering for example an (Al)GaN/InGaN DH structure with an undoped InGaN active layer then the p-type barrier or cladding GaN (or AlGaN) may not have sufficient band offset to confine the holes because of impurity band leakage. Although an active layer that is heavily p-doped may have sufficient confinement, the radiative efficiency might be so low that the threshold becomes too high for lasing.

Experimentally, the impurity conduction can be investigated by Hall measurements. The Hall coefficient for p-type conduction would be

$$R = (p_v \mu_v \mu_{Hv} + p \mu \mu_H) / [e (p_v \mu_v + p \mu)^2],$$

where p_v, μ_v and μ_{Hv} are the carrier density, drift mobility and Hall mobility of the valence band, and p, μ, μ_H are the carrier density, drift mobility and Hall mobility of the impurity band, respectively. The conductivity is then

$$\sigma = e (p_v \mu_v + p \mu).$$

Combined with PL and absorption measurements, a more accurate model of carrier transport can be obtained. We propose systematic p-doping studies along these lines for both GaN and ZnSe.

3. Future plans

i) Based on experimental data (if available), obtain the important parameters of the impurity conduction and impurity band in both GaN and ZnSe based (blue) devices.

ii) Investigate carrier confinement; besides increasing band gap difference, other possible methods are using multi-quantum well barriers (MQB) and/or strain in active layer.

References

[1] Landolt-Bornstein, Data in Science and Technology, Semiconductors Other than Group IV Elements and III-V Compounds, New Series, Springer-Verlag, March 1992.

[2] R.M. Martin, "Relation between elastic tensors of wurtzite and zinc-blende structure materials," Phys. Rev. **B**, 6 (12), pp. 4546, (1972).

[3] N.F. Mott and W.D. Twose, "The theory of impurity conduction," Philos. Mag. Suppl. 10, pp. 107, (1961).

[4] R. Engelmann, "Advances in the State-of-the-Art of GaN Material and Light Emitting Devices," LEOS Newsletter, vol. 8, nr. 5, p.6 (Oct. 1994).

Presentations this quarter

- P.S. Zory gave invited presentation entitled: "Blue-Green Diode Laser Overview" at Kodak in Rochester, NY, Oct. 1994.

- Team gave presentations at the URI Review in Arlington, VA, Oct. 1994.

- P.S. Zory organized and chaired (with the assistance of Diego Olego, Philips Laboratories) the Visible Semiconductor Laser Symposium at the annual meeting of the IEEE/LEOS Society in Boston, MA, Nov. 1, 1994.

- J. Trexler, et.al., "Ohmic Electrical Contacts to p-ZnTe," presented at the 41st National Symposium of the American Vacuum Society in Denver, Colorado, October 24-28, 1994, also accepted for presentation at the Annual Symposium of the Florida Chapter of the AVS in Clearwater Beach, Florida, February 6-8, 1995.

- S. Miller, et.al., "Electrical Contacts to GaN Thin Films," presented at the 41st National Symposium of the American Vacuum Society in Denver, Colorado, October 24-28, 1994; accepted for presentation at the Annual Symposium of the Florida Chapter of the AVS in Clearwater Beach, Florida, February 6-8, 1995, also submitted for presentation at the Materials Research Society Spring Meeting in San Francisco, California, 1995.

- R.M. Park, "High mobility GaN grown by MBE using a rf plasma discharge source," 2nd Workshop on Widegap Nitrides, Oct. 17-18, 1994, St. Louis, MO, Invited talk.

- R.M. Park, "MBE growth of widegap II-VI laser materials: real-time, in-situ monitoring of critical materials properties," IEEE, LEOS '94, Oct. 31 - Nov. 3, 1994, Boston, MA, Invited talk.

Publications during quarter

- G.F. Neumark, L. Radomsky, and I. Kuskovskiy, "Preferential Donor-Acceptor Pairing in Heavily N-doped ZnSe?," accepted, Proc. SPIE.

Publications (Continued)

- Y. Cai and R. Engelmann, "Design of Novel Blue-Green Diode Laser Based on MgZnSeTe Alloy System," accepted for publication in Solid-State Electronics.

- "Dislocations in lattice-mismatched widegap II-VI/GaAs heterostructures as laser light scatterers: experiment and theory," C.M. Rouleau, C.J. Santana, K.S. Jones and R.M. Park, submitted to J. Applied Physics (11/23/94).

Post Doctoral Associates, Graduate Research Assistants, and Undergraduate Research Assistants:

Post Doctoral Associates:

Christopher Walker with Dr. Pankove

Graduate Research Assistants:

Bruce Liu with Dr. Park
Austin Frenkel with Dr. Park
George Kim with Dr. Park
Jeff Hsu with Dr. Zory
Jason O. with Dr. Zory
Igor Kuskovskiy with Dr. Neumark
Li Wang with Dr. Simmons
Y. Cai with Dr. Engelmann
Charles Hoggatt with Dr. Pankove
William A. Melton with Dr. Pankove
John Fijol with Dr. Holloway
T.J. Kim with Dr. Holloway
Jeff Trexler with Dr. Holloway
Steve Miller with Dr. Holloway
Eric Bretschneider with Dr. Anderson
Joe Cho with Dr. Anderson
J. Kim with Dr. Jones
S. Bharatan with Dr. Jones

Undergraduate Research Assistants:

Julie Sauer with Dr. Simmons
Greg Darby with Dr. Park
Bob Covington with Dr. Anderson
Michael Mui with Dr. Anderson
Brendon Cornwell with Dr. Anderson